Static damage identification in beams by minimum constitutive relation error with both full-field and finite-point displacement measurements

A novel static identification approach to beam damage is presented. It is based on the minimum constitutive relation error (CRE) principle where the exact stiffness, the exact displacement and the exact bending moment are shown to make the CRE functional minimal. For practical implementation, two cases regarding full-field displacement measurements and finite-point displacement data, respectively, are considered. For full-field displacement measurements, the CRE functional is directly treated as the objective functional while in case of finite-point measurement data, the CRE functional along with additional penalty terms for treatment of the finite-point displacement measurements is defined as the objective functional. Multiple loads and associated sets of measurements are also considered to improve the identifiability and robustness of the procedure. Convergence is finally verified through numerical examples.

Keywords: damage identification, static measurements, constitutive relation error (CRE), full-field displacement measurement, finite-point displacement measurement

1. Introduction

Damage can arise in structures due to operational incidents, extreme events and/or aggressive environmental conditions. It mainly causes a loss of structural stiffness which may affect the safety, integrity, serviceability and operation of structures. Thus, establishment of the structural health monitoring (SHM) system that provides damage and safety information for preventive maintenance, inspection and repair of structures becomes essential. Indeed, a reliable and effective non-destructive damage identification approach is always the core ingredient of the SHM [1].

There are several conventional, experimental and local approaches that are able to directly identify the damage. The simplest one is visual inspection; however, it is often difficult and even impossible to work well since there may be damage scenarios that are not

visible [2]. Other approaches, such as ultrasonic testing, radiography and thermal analysis, require the damaged region to be known *a priori* and accessible for testing, which cannot be guaranteed in most cases [1]. Hence, global approaches accounting for global behaviour of the damaged region are developed to overcome the difficulties.

Generally, global damage detection approaches are devoted to the identification of damage location and level based on the procedure in which the responses caused by external excitations are measured from dynamic or static tests [3] and thereafter, damage is often identified indirectly through numerical manipulations. A direct consequence of damage is the decrease in local stiffness, and therefore damage, regarded as changes in stiffness, can be detected using changes in dynamic or static characteristics since response characteristics are functions of structural stiffness. This has been the key idea of many extant global approaches [1-5].

In fact, considering the nature of the measured data, global approaches can be classified into two categories: dynamic and static procedures. Due to the convenience in dynamic data measurements, a much larger number of damage identification approaches have been developed based on dynamic tests [6-12]. On the other hand, for certain types of structures, like beam structures, static tests can be performed as easily as dynamic tests. Under this circumstance, the static equilibrium equation is only related to the structural stiffness, and static displacement and strain measurements can be obtained accurately, rapidly and cheaply; while approaches based on dynamic tests often require additional knowledge of mass and damping information, that is to say, the dynamic identification procedure is often complicated due to the uncertainties coming from mass and damping measurements. In spite of the fact, relatively less attention has been paid to static damage identification. Banan and Hjelmstad [13, 14], Viola and Bocchini [15] conducted static parameter identification

through minimizing certain error functions, like least squares fitting errors in displacements or equilibrium equations, based on finite element models. Di Paola and Bilello [2] identified damage in beams through an integral equation. Ghrib [16] investigated the efficiency of two computational procedures—equilibrium gap formulation and minimization of a data-discrepancy functional—for damage detection using static responses. Avril and Pierron [17] proposed a virtual field method for identification of constitutive parameters. Yang and Sun [18], Rezaiee-Pajand et al. [19] localized and quantified structural damage through sensitivity analysis of the stiffness to finite element equilibrium equations. Caddemi and Greco [20], Abdo [3], Bakhtiari-Nejad et al. [21] analysed the influence of measurement noises, number and spatial distribution of measured data and character of load cases.

In the present paper, damage identification is performed based on static test data through a minimum constitutive relation error (CRE) procedure which is quite different from the error function approaches in [13-15, 22]. The idea is enlightened by a recent variational theory of Geymonat and Pagano [23] for inverse parameter identification that the CRE function is convex and its minimization can lead to a well-posed problem. As they pointed out, constitutive parameters and stresses can be identified through minimization of the CRE as long as displacement measurements are readily acquired under given loads. The conclusion reached by the theory is very attractive and as a first attempt to implement the theory, a constitutive equation gap method has been proposed very recently by Florentin and Lubineau [24-27] for parameter identification in plane elasticity problems. However, as indicated in the theory, the complete and comprehensive application requires the full-field/global displacement measurements along with a complementary-energy-based solver for stresses which is not yet applicable to general two- and three- dimensional

problems [28, 29]. Notwithstanding, the method is quite tailored for beam structures in the following two aspects:

(1) global displacement measurements are easily available, and

(2) the standard force method [30] based on the minimum complementary energy principle is easily conducted and it often requires substantially less degrees of freedom than conventional displacement-based finite element models.

That is to say, the minimum CRE theory is completely applicable to damage identification in beam structures, to which this paper is just devoted. Considering that getting the measurement data is of vital importance for practical identification and different measurement techniques often correspond to different identification procedures, a number of commonly-used and developing measurement techniques and their recent development are additionally reviewed in what follows.

Traditionally, for static measurements, displacements including deflections and slopes of beams are measured at finite points using linear variable-differential transformers (LVDT) [16] reliable up to 10^{-6}mm [31] accuracy and global positioning systems (GPS) [32, 33], with absolute errors down to a few millimetres in practice. For damage identification corresponding to these finite-point measurement techniques, the accuracy of identification results depends mainly on the amount and locations of the sensors.

On the other hand, with fast development of computer-based technologies and digital imaging devices, laser and other light sources, optical-based measurement techniques [34] open up a new possibility in quasi-continuous measurement of structures at an affordable cost; these include (but are not limited to) the digital image processing techniques [35], the laser scanning [36, 37] and the interferometry [38]. Particularly, the digital image processing

techniques, such as digital image correlation [39], close-range digital photogrammetry [40], image edge detection [41], optical flow method/principle [42, 43], have exhibited their powerful measurement abilities in various experiments. Results even showed that the relative error between the displacements measured by these techniques and the exact values can be less than 0.5% [44]. In addition, prior researches have shown that the full-field displacements could be appropriately rebuilt through a sufficient number of displacement data along with some suitable data pre-processing algorithms [45]. For more optical-based measurement techniques in both static and dynamic engineering applications, refer to [38, 41, 42, 46-53].

In this paper, damage identification in beams is performed using either the finite-point measurements by the traditional LVDT or the quasi-continuous measurements by the optical-based techniques. The primary objective is to identify the damaged stiffness $k \in \mathrm{C}$ as well as bending moment $M \in \Im$, under the full-field displacement measurements $w \in \mathrm{U}$, e.g., obtained by optical-based techniques and the respective static loading conditions $\Im$ where C, U, $\Im$ represent the admissible material, displacement and bending moment spaces, respectively. The basic inverse identification problem reads: find $(k, M) \in \mathrm{C} \times \Im$ with given $w \in \mathrm{U}$, which is a reverse of the forward problem: find $(w, M) \in \mathrm{U} \times \Im$ with known $k \in \mathrm{C}$. Evidently, by solving the inverse problem, one can not only identify the damage, but also reconstruct the stiffness and bending moment distribution. Moreover, the objective is also enriched to tackle damage identification using finite-point displacement measurements. By this way, the static damage identification procedure becomes more adjustable to traditional measurement techniques, e.g., the LVDT for which finite-point displacement measurements are often obtained.

The remainder of the paper is organized as follows. The inverse identification problem for a Bernoulli-Euler beam model is simply introduced in Section 2. In Section 3,

the minimum CRE principle for inverse identification is presented for full-field displacement measurements and then, modification is invoked to cope with finite point measurements. Practical implementation and convergence of the proposed approach are discussed elaborately in Section 4. Numerical tests are performed in Section 5 and final conclusions are drawn in Section 6.

2. Problem statement

Consider a one-dimensional Bernoulli-Euler beam defined in interval $X=[x_s,x_e]$ as shown in **Fig. 1**. The flexural stiffness of the beam is assumed to be $k(x)=EI(x)$. Loading conditions are distributed loads $q(x)$ and concentrated loads F^{ex},M^{ex} along with boundary displacements w_p on the prescribed displacement boundary Σ. In this beam model, the bending moment M is directly related to the curvature through the constitutive relation $M=k\theta'=kw''$ and the shear force V is given by $V=M'$. For general equilibrium, $V'=M''=q(x)$ and V,M should be in equilibrium with concentrated loads. The beam model can be described as a combination of the following three parts:

- Kinematic constraints

$$\mathrm{U}=\{w\in H^2(X):\ w=w_p \text{ on } \Sigma\} \tag{1}$$

- Equilibrium equations

Find bending moment $M\in\Im$ with

$$\Im=\{M:V=M',M''=q(x),V \text{ and } M \text{ are in equilibrium with } F^{ex} \text{ and } M^{ex}\}, \tag{2}$$

or

$$\Im = \{M \in L_2(X) : \int_X Mv''dx = \int_X q(x)vdx + \sum (F^{ex}v(x^{ex}) + M^{ex}v'(x^{ex})), \forall v \in \mathrm{U}_0\} \tag{3}$$

with x^{ex} denoting the position where concentrated loads F^{ex}, M^{ex} are enforced and U_0 the homogeneous part of U;

- Constitutive relation

$$M = kw'' \tag{4}$$

with $k \in \mathrm{C} \triangleq \{k \in L_2(X) : \exists 0 < c_0 < C_0, \text{ such that } c_0 \le k(x) \le C_0\}$ representing a positive and bounded stiffness field.

Generally, $\mathrm{U}, \Im, \mathrm{C}$ that will be used frequently in what follows are called the spaces of (kinematically) admissible displacement field, (statically) admissible bending moment field and (constitutively) admissible elastic stiffness field, respectively.

3. The minimum CRE principle for inverse identification

3.1 CRE functional

Consider an admissible solution trio $(\tilde{w}, \tilde{M}, \tilde{k})$ which satisfies

$$\tilde{w} \in \mathrm{U}, \tilde{M} \in \Im, \tilde{k} \in \mathrm{C}. \tag{5}$$

It is easily known that if the constitutive relation (4) is additionally satisfied, the solution trio would be the exact solution of the Bernoulli-Euler beam model. Thus, to measure the distance of the admissible solution trio to the exact solution trio in energy product, an error in constitutive relation is introduced

$$e_{CRE}(\tilde{w}, \tilde{M}, \tilde{k}) = \frac{1}{2}\int_X \frac{(\tilde{M} - \tilde{k}\tilde{w}'')^2}{\tilde{k}} dx \tag{6}$$

which is termed the constitutive relation error (CRE) [54, 55] (or constitutive equation gap (CEG) [24].

3.2 Identification through minimum CRE

In practice, damage identification approaches appear to be limited with respect to certain displacement measurement techniques. Herein, two cases regarding full-field displacement measurements and finite-point displacement data, respectively, are considered within the framework of the minimum CRE theory. For the first case using full-field displacement measurements, the CRE functional (6) is directly treated as the objective functional and the parameter identification approach is referred to as the min-CRE approach; while in case of finite-point measurement data, the CRE functional along with additional penalty terms for treatment of the finite-point displacement measurements are defined as the objective functional. The second identification case is more applicable and can be viewed as extension of the first identification case. Therefore, the identification approach involved in the second case is referred to as the modified min-CRE approach.

3.2.1 Min-CRE approach

Assume that the spaces C, U and $\Im$ for search of the stiffness k, displacement w and the bending moment M, respectively, are already known. Then, identification of the stiffness k as well the bending moment M from the full-field displacement data $\hat{w}$ pertains to the following minimization of the CRE functional (6), i.e.,

$$(M,k) = \arg \min_{\tilde{M}\in\Im,\tilde{k}\in\mathrm{C}} F(\tilde{M},\tilde{k});\ F(\tilde{M},\tilde{k}) := e_{CRE}(\tilde{M},\tilde{k},\hat{w}), \tag{7}$$

which is known as the minimum CRE principle [23] for inverse identification. To proceed

further, it is necessary to clarify some important properties of the CRE function $F(\cdot,\cdot,\cdot)$.

- Theorem 1

The following properties for $F(\cdot,\cdot)$ on compact spaces $\Im\times\mathrm{C}$ hold:

(a) $F(\tilde{M},\tilde{k})\geq 0$, $\forall(\tilde{M},\tilde{k})\in\Im\times\mathrm{C}\times\mathrm{U}$.

(b) $F(\tilde{M},\tilde{k})=0$ if and only if the constitutive relation $\tilde{M}=\tilde{k}\hat{w}''$ is verified.

(c) The functional $F(\cdot,\cdot)$ is convex on $\Im\times\mathrm{C}$.

(d) The convexity of $F(\cdot,\cdot)$ on $\Im\times\mathrm{C}$ guarantees the existence of the minimizer to problem (7). Then, if $\mu(x\in X:\hat{w}''(x)=0)=0$ with $\mu(\cdot)$ denoting the Lebesgue measure, the minimizer must lie in $\Im^*\times\mathrm{C}$ with $\Im^*=\{M\in\Im:\mu(x\in X:M(x)=0)=0\}$ and moreover, $F(\cdot,\cdot)$ possesses separately strict convexity on $\Im^*\times\mathrm{C}$.

Detailed proof of the Theorem 1 is given in Appendix. According to Theorem 1, it is seen that the damaged stiffness is identifiable through the minimum CRE principle in beams. Theoretically, the complete and unique identification of the damage requires some extra conditions on the static measurements—which are inherent in the context of inverse problems (see Remark 1 in Appendix)—including the deforming condition $\mu(\hat{w}''(x)=0,x\in X)=0$ such that $F(\cdot,\cdot)$ becomes strictly convex in the vicinity of the minimizer.

In practice, using more than one set of static measurements could improve the identifiability and robustness of the identification procedure and provide remedy for possible unidentifiability of the proposed approach [31, 56]. To this end, the objective functional as well as the identification procedure becomes,

$$(M^{(1)},M^{(2)},...,k)=\arg\min_{\tilde{M}^{(j)}\in\Im^{(j)},\tilde{k}\in\mathrm{C}}F(\tilde{M}^{(1)},\tilde{M}^{(2)},...,\tilde{k});$$
$$F(\tilde{M}^{(1)},\tilde{M}^{(2)},...,\tilde{k}):=\sum_j r_j e_{CRE}(\tilde{M}^{(j)},\tilde{k},\hat{w}^{(j)}) \quad (8)$$

where $\hat{w}^{(j)}$ denotes the jth set of full-field displacement data resulting from the loading condition $\tilde{M}^{(j)}\in\Im^{(j)}$ and $r_j\geq 0$ is the corresponding weighting coefficient and $\sum_j r_j=1$. The selection of weighting coefficient r_j is determined by the reliability of practical measurements: if $(w_{\mathrm{m}},\Im_{\mathrm{m}},\mathrm{U}_{\mathrm{m}})$ is more reliable than $(w_n,\Im_n,\mathrm{U}_n)$, r_{m} would be selected to be greater than r_{n}; else it would be otherwise. Generally, r_{m} and r_{n} are taken equally. It is evidently seen that as long as $\sum_j r_j(w_j'')^2\neq 0$ on $X_i,\forall i=1,2,...,n$, the constitutive-relation step for k_i can proceed.

3.2.2 Modified min-CRE approach

In most cases, finite-point displacement measurements rather than full-field displacement measurements are available. Let $\{\hat{w}_i,i\in\wp\}$ be the measured finite-point displacement data on the set of points $\{i\in\wp\}$ and then, a new objective functional as well as a new parameter identification formulation is given as follows.

$$F_{\mathrm{mod}}(\tilde{M},\tilde{k},\tilde{w}):=e_{CRE}(\tilde{M},\tilde{k},\tilde{w})+\sum_{i\in\wp}\frac{A_i}{2}|\tilde{w}_i-\hat{w}_i|^2$$
$$(M,w,k)=\arg\min_{\tilde{M}\in\Im,\tilde{w}\in\mathrm{U},\tilde{k}\in\mathrm{C}}F_{\mathrm{mod}}(\tilde{M},\tilde{k},\tilde{w}); \quad (9)$$

where w_i is the displacement of w at point i and $\{A_i>0,i\in\wp\}$ represent the penalty factors. Practically, values of $\{A_i>0,i\in\wp\}$ could be tuned according to the confidence of the corresponding displacement data: $A_i\to+\infty$ means completely trust of this data, while

$A_i \to 0$ means completely untrust. Again, in case of multiple sets of static data, the parameter identification can read,

$$(M^{(1)}, w^{(1)}, M^{(2)}, w^{(2)}, ..., k) = \arg \min_{\tilde{M}^{(j)} \in \Im^{(j)}, \tilde{w}^{(j)} \in \mathrm{U}^{(j)}, \tilde{k} \in \mathrm{C}} F_{\mathrm{mod}}(\tilde{M}^{(1)}, \tilde{w}^{(1)}, \tilde{M}^{(2)}, \tilde{w}^{(2)}, ..., \tilde{k});$$
$$F_{\mathrm{mod}}(\tilde{M}^{(1)}, \tilde{w}^{(1)}, \tilde{M}^{(2)}, \tilde{w}^{(2)}, ..., \tilde{k}) := \sum_j r_j [e_{CRE}(\tilde{M}^{(j)}, \tilde{k}, \tilde{w}^{(j)}) + \sum_{i \in \wp} \frac{A_i}{2} \left| \tilde{w}_i^{(j)} - \hat{w}_i^{(j)} \right|^2] \quad (10)$$

where $\Im^{(j)}, \mathrm{U}^{(j)}$ represents the loading and prescribed displacement boundary conditions for the *j*th set of static measurement, $\hat{w}_i^{(j)}$ is the corresponding measurement displacement at point *i* and r_j is the weight.

In what follows, specific algorithms will be elaborately designed to solve the minimization problems (7)-(10).

4. Practical implementation

Section 3 gave the theoretical view that the damaged stiffness can be identified through the minimum CRE principle. In this section, numerical algorithms for the min-CRE approach and the modified min-CRE approach are to be developed.

4.1 Min-CRE approach

In Theorem 1, the CRE function is shown to be convex and hence, separately convex on $\tilde{M}$ and $\tilde{k}$. Thus, for practical implementation, a two-step substitution algorithm is developed as follows:

Firstly, minimization of the CRE function over $\tilde{M}$ yields a minimum complementary energy problem that should be solved by the force method. Therefore, the procedure is simply designated as

$$\begin{aligned}\tilde{M} &= Force\_Method(\tilde{k}, \Im, \mathrm{U}) \\ &:= \arg\min_{\tilde{M}\in\Im}\left\{\frac{1}{2}\int_X \frac{\tilde{M}^2}{\tilde{k}}dx - \sum\nolimits_p (\theta_p \tilde{M}\,|_p - w_p(\tilde{M})'\,|_p)\right\}\end{aligned} \tag{11}$$

and this step is called the force-method step.

Secondly, minimization of the CRE over $\tilde{k}$ gives

$$\int_X \left\{\frac{\tilde{M}^2}{\tilde{k}^2} - (w'')^2\right\}\delta\tilde{k}dx = 0. \tag{12}$$

Practically, it is sufficient to assume that the stiffness $\tilde{k}$ is piecewise constant, that is to say,

$$\begin{aligned}&X = \bigcup_{i=1}^N X_i, \forall 1 \le i \ne j \le N, X_i \text{ and } X_j \text{ are non-overlapping,} \\ &\tilde{k}(x) = \{\tilde{k}_i, x \in X_i\}\end{aligned} \tag{13}$$

where N is the number of non-overlapping pieces, or elements. **Eq. (12)** means that the equation in the parenthesis must be zero at every point due to any variation of stiffness. Under the piecewise constant assumption of the stiffness and due to any variation of piecewise constant stiffness, **Eq. (12)** is reduced to

$$\sum_i \int_{X_i}\left\{\frac{\tilde{M}^2}{\tilde{k}_i^2} - (w'')^2\right\}\delta\tilde{k}_i dx = 0 \Leftrightarrow \int_{X_i}\left\{\frac{\tilde{M}^2}{\tilde{k}_i^2} - (w'')^2\right\}dx = 0,\ i = 1,2,...,N \tag{14}$$

and then, one has

$$\tilde{k}_i = \sqrt{\frac{\int_{X_i}\tilde{M}^2 dx}{\int_{X_i}(w'')^2 dx}}, i = 1,2,...,N. \tag{15}$$

It turns out that **Eq. (15)** looks like the direct use of the constitutive relation in Eq. (4). Thus, this step is named the constitutive-relation step.

After integration of both **Eqs. (11) and (15)**, a two-step iterative algorithm for the min-CRE approach is established for its convenience to solve sets of equations. Actually, the

two-step substitution algorithm is designed for solution of the discrete version of the problem (8); that is

$$(M_h, k_h) = \arg \min_{\tilde{M}_h \in \Im, \tilde{k}_h \in C_h} F(\tilde{M}_h, \tilde{k}_h) \tag{16}$$

where $C_h = \{k \in C : k \text{ is constant in } X_i, i = 1,2,...,N\}$ is a compact subspace of C. Finally, as closure of this subsection, the two-step substitution algorithm will be shown to converge for problem (16).

- Theorem 2

Assume that the problem (16) has a unique minimizer (M_h, k_h) and $F(\cdot,\cdot)$ is strictly convex in the vicinity of (M_h, k_h), then, the two-step substitution algorithm will converge to the exact solution.

The specific proof is exhibited in Appendix. The convergence theorem above is for the min-CRE approach using only one set of static measurement data, nevertheless, it can be easily extended to the min-CRE approach with more than one set of static measurements and the modified-CRE approach; these will not be specified any more. As regards the case of more than one set of static measurements, a similar algorithm can be established as shown in **Table 1**.

Table 1 A two-step substitution algorithm for min-CRE approach under multiple sets of static measurements *w*

• Given the initial stiffness k^0 and the initial bending moment $M^{(1)0}, M^{(2)0}, \ldots,$ i.e.

$M^{(1)0} = Force\_Method(k^0, \Im^{(1)}, \mathrm{U}^{(1)})$,
$M^{(2)0} = Force\_Method(k^0, \Im^{(2)}, \mathrm{U}^{(2)})$,
...

- Successively determine $\left(k^{n+1}, M^{(1)n+1}, M^{(2)n+1}, ...\right)$ from $\left(k^n, M^{(1)n}, M^{(2)n}, ...\right)$ by the following two steps,

step 1: $k^{n+1} = \{\sqrt{\dfrac{\int_{X_i} \sum_j r_j (M^{(j)n})^2 dx}{\int_{X_i} \sum_j r_j (w^{(j)\prime\prime})^2 dx}}, x \in X_i, i = 1, 2, ..., N\}$,

step 2: $M^{(1)n+1} = Force\_Method(k^{n+1}, \Im^1, \mathrm{U}^1)$,
$M^{(2)n+1} = Force\_Method(k^{n+1}, \Im^2, \mathrm{U}^2)$,
...

- Test of convergence with given error tolerance TOL,

$$\sqrt{\frac{\int_X (k^{n+1} - k^n)^2 dx}{\int_X (k^0)^2 dx}} + \sqrt{\frac{\int_X (M^{(1)n+1} - M^{(1)n})^2 dx}{\int_X (M^{(1)0})^2 dx}} + \sqrt{\frac{\int_X (M^{(2)n+1} - M^{(2)n})^2 dx}{\int_X (M^{(2)0})^2 dx}} + ... \le \mathrm{TOL}$$

4.2 Modified min-CRE approach

Turning to the modified CRE functional (9), it is found that minimization over $\tilde{k}$ would result in the same constitutive-relation step (15) with those in the min-CRE approach. The difference lies in the introduction of a new unknown quantity w. Minimization of the CRE functional (9) over $\tilde{M}$ and $\tilde{w}$ yields

$$\int_X \delta\tilde{M} \left(\frac{\tilde{M}}{\tilde{k}} - \tilde{w}'' \right) dx + \int_X \delta\tilde{w}'' \left(\tilde{k}\tilde{w}'' - \tilde{M} \right) dx + \sum_{i \in \wp} A_i \delta\tilde{w}_i (\tilde{w}_i - \hat{w}_i) = 0 \qquad (17)$$

where $\tilde{M} = \tilde{M}_r + \hat{M}_P$ with $\tilde{M}_r = \boldsymbol{N}_r \tilde{\boldsymbol{F}}_r$ being the bending moment produced by the unknown redundant forces $\tilde{\boldsymbol{F}}_r$ and the corresponding shape functions $\boldsymbol{N}_r$, and $\hat{M}_p = \boldsymbol{N}_p \hat{\boldsymbol{F}}_p$ the bending

moment caused by the given external loads $\hat{\boldsymbol{F}}_p$ and the corresponding shape functions $\boldsymbol{N}_p$.

Base on this, **Eq. (17)** could be rearranged into

$$\int_X \begin{pmatrix} \delta\tilde{M}_r \\ \delta\tilde{w}'' \end{pmatrix}^T \begin{pmatrix} \frac{1}{\tilde{k}} & -I \\ -I & \tilde{k} \end{pmatrix} \begin{pmatrix} \tilde{M}_r \\ \tilde{w}'' \end{pmatrix} dx + \sum_{i\in\wp} A_i \begin{pmatrix} \delta\tilde{M}_r \\ \delta\tilde{w}_i \end{pmatrix}^T \begin{pmatrix} 0 \\ \tilde{w}_i \end{pmatrix} = \sum_{i\in\wp} A_i \begin{pmatrix} \delta\tilde{M}_r \\ \delta\tilde{w}_i \end{pmatrix}^T \begin{pmatrix} 0 \\ \hat{w}_i \end{pmatrix} + \int_X \begin{pmatrix} \delta\tilde{M}_r \\ \delta\tilde{w}'' \end{pmatrix}^T \begin{pmatrix} -\frac{1}{\tilde{k}} \\ I \end{pmatrix} \hat{M}_p dx \quad (18)$$

where I is the identify operator.

Furthermore, the displacement field $\tilde{w}$ is often represented by the cubic Hermite interpolation of nodal deflections $\{w_j\}$ and slopes $\{\theta_j\}$ and the curvature field $\tilde{w}''$, accordingly, is approximated by the second derivative of cubic Hermite interpolation of nodal deflections $\{w_j\}$ and slopes $\{\theta_j\}$. In other words, for an arbitrary element e with two nodes i,j whose coordinates are $x_i<x_j$, the following approximation is adopted,

$$\begin{aligned} &\tilde{w} = \begin{pmatrix} H_1 & H_2 & H_3 & H_4 \end{pmatrix} \tilde{\boldsymbol{V}}^e \\ &\tilde{w}'' = \begin{pmatrix} H''_1 & H''_2 & H''_3 & H''_4 \end{pmatrix} \tilde{\boldsymbol{V}}^e, \tilde{\boldsymbol{V}}^e = \begin{bmatrix} w_i, & \theta_i, & w_j, & \theta_j \end{bmatrix} \end{aligned} \quad (19)$$

where the functions H_1, H_2, H_3, H_4 are of the following forms

$$\begin{aligned} &H_1(\xi) = \frac{1}{2}(\xi+2)(\xi-1)^2, H_2(\xi) = \frac{1}{4}(\xi+1)(\xi-1)^2 \frac{h^e}{2} \\ &H_3(\xi) = \frac{1}{2}(2-\xi)(\xi+1)^2, H_4(\xi) = \frac{1}{4}(\xi-1)(\xi+1)^2 \frac{h^e}{2} \\ &h^e = x_j - x_i, \xi = \frac{2(x-x_i)}{h^e} - 1. \end{aligned} \quad (20)$$

For brevity, the total finite element approximation to the displacement and curvature field is designated as

$$\tilde{w} = \boldsymbol{H}\tilde{\boldsymbol{V}}, \quad \tilde{w}'' = \boldsymbol{H}''\tilde{\boldsymbol{V}} \quad (21)$$

where $\boldsymbol{H}$ forms the finite element space and $\tilde{\boldsymbol{V}}$ collects all the displacement DOFs.

Above all, **Eq. (18)** can yield,

$$\begin{pmatrix} \mathbf{S} & -\mathbf{C} \\ -\mathbf{C}^{\mathrm{T}} & \mathbf{K} \end{pmatrix}\begin{pmatrix} \tilde{\boldsymbol{F}}_r \\ \tilde{\boldsymbol{V}} \end{pmatrix}=\begin{pmatrix} \mathbf{a} \\ \mathbf{b} \end{pmatrix}$$

$$\mathbf{S}=\int_X \boldsymbol{N}_r^T \frac{1}{k}\boldsymbol{N}_r \mathrm{d}x$$

$$\mathbf{K}=\int_X \boldsymbol{H}''^T k\boldsymbol{H}''\mathrm{d}x+\mathbf{A}, \mathbf{A} \text{ a diagonal mtrix with } \mathbf{A}(i,i)=\begin{cases} A_i, i\in\wp \\ 0, i\notin\wp \end{cases}; \quad (22)$$

$$\mathbf{C}=\int_X \boldsymbol{N}_p{}^T \boldsymbol{H}''\mathrm{d}x$$

$$\mathbf{a}=-\int_X \boldsymbol{N}_r^T \frac{1}{k}\hat{M}_p \mathrm{d}x, \mathbf{b}=\int_X \boldsymbol{H}''^T \hat{M}_p \mathrm{d}x+\mathbf{p},\ \mathbf{p}(i)=\begin{cases} A_i\hat{w}_i, i\in\wp \\ 0, i\notin\wp \end{cases}$$

This step is called the displacement/force-recovery step which is designated to recover full-field displacement and bending moment data from incomplete finite-point displacement data. For simplicity, this step is designated as $(M,w)=recovery(\tilde{k},\Im,\mathrm{U},\{\hat{w}_i,i\in\wp\})$.

As a consequence, a similar two-step iterative algorithm (to that in **Table 1**) for the modified min-CRE approach with multiple sets of measurement data can be established in **Table 2**.

Table 2 A two-step substitution algorithm for modified min-CRE approach under multiple sets of static measurements *w*

- Given the initial stiffness k^0, the initial displacements $w^{(1)0}, w^{(2)0},...$ and the initial bending moments $M^{(1)0}, M^{(2)0},...$, i.e.

  $(M^{(1)0}, w^{(1)0})=recovery(k^0,\Im^{(1)},\mathrm{U}^{(1)},\{\hat{w}_i^{(1)},i\in\wp\})$,
  $(M^{(2)0}, w^{(2)0})=recovery(k^0,\Im^{(2)},\mathrm{U}^{(2)},\{\hat{w}_i^{(2)},i\in\wp\})$,
  .....

- Successively determine $\left(k^{n+1}, M^{(j)n+1}, w^{(j)n+1}\right)$ from $\left(k^n, M^{(j)n}, w^{(j)n}\right)$ by the following two steps,

step 1: $k^{n+1} = \left\{ \sqrt{\dfrac{\int_{X_i} \sum_j r_j (M^{(j)n})^2 dx}{\int_{X_i} \sum_j r_j (w^{(j)n''})^2 dx}}, x \in X_i, i = 1,2,...,N \right\}$,

step 2: $(M^{(1)n+1}, w^{(1)n+1}) = recovery(k^{n+1}, \Im^{(1)}, \mathrm{U}^{(1)}, \{\hat{w}_i^{(1)}, i \in \wp\})$,
$(M^{(2)n+1}, w^{(2)n+1}) = recovery(k^{n+1}, \Im^{(2)}, \mathrm{U}^{(2)}, \{\hat{w}_i^{(2)}, i \in \wp\})$,
.....

- Test of convergence with given error tolerance TOL,

$$\sqrt{\frac{\int_X (k^{n+1} - k^n)^2 dx}{\int_X (k^0)^2 dx}} + \sqrt{\frac{\int_X (M^{(1)n+1} - M^{(1)n})^2 dx}{\int_X (M^{(1)0})^2 dx}} + \sqrt{\frac{\int_X (M^{(2)n+1} - M^{(2)n})^2 dx}{\int_X (M^{(2)0})^2 dx}} + ...$$
$$+ \sqrt{\frac{\int_X (w^{(1)n+1} - w^{(1)n})^2 dx}{\int_X (w^{(1)0})^2 dx}} + \sqrt{\frac{\int_X (w^{(2)n+1} - w^{(2)n})^2 dx}{\int_X (w^{(2)0})^2 dx}} + ... \le \mathrm{TOL}$$

5. Numerical tests

To show the effectiveness of the proposed damage identification approach, three beams are studied. They are a propped cantilever beam, a simply supported beam and a three-span continuous beam, respectively. For application of the two-step substitution algorithm (in **Tables 1** and **2**), the convergence tolerance is practically set to $\mathrm{TOL} = 1 \times 10^{-6}$.

5.1 Example 1—a propped cantilever beam

A propped cantilever beam of continuously varying stiffness $k(x) = k_0(1 + x/L)^2$ with $k_0 = 1$ (see **Fig. 2)** is studied in this example to examine the capacity and identifiability of the proposed min-CRE approach for damage identification in general beams. The geometric parameter is $L = 1$. The deflection was measured at 24 equally spaced positions along the beam, each of which was 0.04 between two adjacent locations.

To show the effectiveness of multiple sets of load patterns/static measurements and its influence on the number of elements adopted, different loading cases are considered for this propped cantilever beam: the beam is uniformly partitioned into 25 elements under single load pattern and two load patterns, 50 elements under two load patterns, 100 elements under two load patterns and three load patterns and 200 elements under three load patterns. Three sets of load patterns are used herein: a concentrated moment $M_0 = 1$ at the right end, a unit concentrated force at $x = 0.3$ and a concentrated moment $M_0 = 1$ at $x = 0.3$, as shown in **Fig. 2**. The load pattern is selected randomly for the case with single load pattern or two load patterns. Displacements under each load pattern are obtained directly from analytical solution without noise.

The algorithm in **Table 1** is adopted with an initial stiffness being $k^0(x) = 1$. Eventually, the piecewise stiffness can be identified as exhibited in **Fig. 3**. As we can see, as the number of elements increases, the introduction of additional sets of load patterns can help to improve and enhance the identifiability of the algorithm. Limited sets of load patterns and large number of elements to be identified, such as the case of 25 elements under single load pattern and 100 elements under two load patterns, might lead to the perturbation and deviation in the identification results. In fact, this conclusion not only provides remedy for possible unidentifiability of the proposed approach, but also is inherent in all inverse identification problems.

In addition, to show the convergence of the proposed min-CRE approach, the bending moment at the left end of the beam $M(x = 0)$ is observed at each iteration step. Detailed results are displayed in **Fig. 4**. It is seen that the bending moment converges only after 20 iterations, verifying the convergence of the two-step substitution algorithm.

5.2 Example 2—a simply supported experimental beam

In this example, experimental finite-point measurements are used for stiffness identification to testify the applicability of the modified min-CRE approach. The beam model is taken from the experimental bending test in [57]. Parameters of the experimental uniform beam are: length $L = 4\,\mathrm{m}$, Young's modulus $E = 206\,\mathrm{GPa}$ and the H-$100\times100\times6/8$ section with depth of 100mm, flange width of 100mm, web thickness of 6mm and flange thickness of 8mm. Only one load case is enforced in the experiment with a concentrated force P=9.66kN at the middle point of the beam as shown in **Fig. 5**. Experimental displacements attained by the LVDT and the Terrestrial Laser Scanning (TLS) [57] are shown in **Fig. 5**. Using these displacement data, the distributive stiffness of the beam can be identified by the modified min-CRE approach and detailed results are presented in **Fig. 6**. The value of the initial uniform second moment of area is set to $400\mathrm{cm}^4$. Obviously, the distributive stiffness is well identified with respect to the beam's theoretical second moment of area $383\mathrm{cm}^4$ (**Fig. 6**); the relative errors are less than 3% for both the LVDT data and the TLS data.

5.3 Example 3—a three-span continuous beam

Damage in an equi-spaced three-span continuous and statically indeterminate beam (see **Fig. 7**) is to be identified in this example. The length of each span is $L = 2\,\mathrm{m}$ and the stiffness of the intact beam over the whole beam is $k^0 = 8.33\times10^4\,\mathrm{N\cdot m}^2$. In this numerical test, measurement points are so distributed that each span is uniformly partitioned into four elements and the specific enumeration of points and elements are also shown in **Fig. 7**.

Two damage cases are taken into account, including:

- Small damage case D1: stiffness reduced to 95%, 90% and 85% in elements 1, 4 and 10, respectively; and

- Large damage case D2: stiffness reduced to 60%, 40% and 80% in elements 1, 4 and 10, respectively.

To enhance the identifiability of the algorithm, nine sets of load cases are considered and for each case, a concentrated force is enforced on one of the nodes 2-4, 6-8 and 10-12. Accordingly, nine sets of static displacements at the same nine points are measured. This kind of measurement can often be seen in damage detection of bridges for which a moving truck (or load) is used to generate the multiple load cases.

The simulated displacement data are acquired through finite element computation. A uniform distribution noise is added to the simulated response as

$$\text{noise}(x) = uniform \cdot a \tag{23}$$

where $uniform$ is a number pertains to the uniform distribution and a is the applied noise level. Noise of level 0.1mm is considered in this example.

For the sake of convenience, the damage index DAI is introduced to represent the scaled damage in the beam, i.e.

$$\text{DAI}_i = k_i^{damage} / k_i^0 \tag{24}$$

for the ith element where k_i^{damage} is the damaged stiffness in element i.

By performing the iterative algorithm in **Table 2** with the initial stiffness setting to the stiffness of the intact beam, the min-CRE approach and modified min-CRE approach for damage identification could proceed. To get a better picture for the cases with noise, statistical analysis was performed. Mean values and standard deviations of DAI over 50 Monte Carlo trials are presented in **Fig. 8**. It is clear that the modified min-CRE approach greatly improves the identifiability and robustness of the min-CRE approach in terms of the

mean values and standard deviation of DAI. To visualize the convergence of the algorithm for large damage case D2, detailed results on the DAI (see **Eq.(24)**) at each iteration step are given in **Fig. 9**. Obviously, all the quantities converge within 200 iterations and this verifies the convergence of the proposed two-step substitution algorithm. The displacement fields for the large damage case D2 are also rebuilt based on this approach. As can be seen from Fig. 10, the 'uncertainties' due to the noise in the discrete displacement boundary are much more overcome in these superior rebuilt fields, which results in good identification for the damage.

6. Conclusions

Two new approaches based on the minimum constitutive relation error (CRE) principle have been proposed for static damage identification in Bernoulli-Euler beams, i.e. the min-CRE approach for full-field measurements and the modified min-CRE approach for finite-point measurements, respectively. The difference between the two approaches is whether to use additional penalty terms for enforcement of the experimental displacement data or not. A two-step iterative strategy has been established to fulfil the practical implementation and its convergence has been proved. The robustness of these approaches could be guaranteed by applying multiple sets of static measurements. Numerical tests have been carried out to verify these approaches. The sound performance of these proposed approaches in the following aspects have been observed:

(1) The approaches are well applicable to both statically determinate and indeterminate beam structures for stiffness/damage identification and bending moment reconstruction;

(2) The objective function of these approaches is (separately) convex and large damages could be well identified;

(3) The approaches perform well under measurement noise;

(4) The approaches converge well in practice.

Therefore, it is believed that the proposed approach can serve as an effective tool for practical structural damage identification.

Acknowledgements:

The authors are grateful to Professor Hongzhi Zhong of Tsinghua University for the valuable comments for revision. The present investigation was performed under the support of the National Natural Foundation of China (Nos. 51178247 and 51378294) and the MEXT scholarship of Japan.

References

[1]. Fan W, Qiao P. Vibration-based damage identification methods: a review and comparative study. Structural Health Monitoring. 2011;10:83-111.

[2]. Di Paola M, Bilello C. An integral equation for damage identification of Euler-Bernoulli beams under static loads. Journal of Engineering Mechanics. 2004;130:225-34.

[3]. Abdo MA-B. Parametric study of using only static response in structural damage detection. Engineering Structures. 2012;34:124-31.

[4]. Huynh D, He J, Tran D. Damage location vector: A non-destructive structural damage detection technique. Computers & Structures. 2005;83:2353-67.

[5]. Sung S, Jung H, Jung H. Damage detection for beam-like structures using the normalized curvature of a uniform load surface. Journal of Sound and Vibration. 2013;332:1501-19.

[6]. Abdo M-B, Hori M. A numerical study of structural damage detection using changes in the rotation of mode shapes. Journal of Sound and Vibration. 2002;251:227-39.

[7]. Cornwell P, Doebling SW, Farrar CR. Application of the strain energy damage detection method to plate-like structures. Journal of Sound and Vibration. 1999;224:359-74.

[8]. Debruyne S, Vandepitte D, Moens D. Identification of design parameter variability of honeycomb sandwich beams from a study of limited available experimental dynamic structural response data. Computers & Structures. 2015;146:197-213.

[9]. Greco A, Pau A. Damage identification in Euler frames. Computers & Structures. 2012;92:328-36.

[10]. Pandey A, Biswas M. Damage detection in structures using changes in flexibility. Journal of Sound and Vibration. 1994;169:3-17.

[11]. Pandey A, Biswas M, Samman M. Damage detection from changes in curvature mode shapes. Journal of Sound and Vibration. 1991;145:321-32.

[12]. Salawu O. Detection of structural damage through changes in frequency: a review. Engineering Structures. 1997;19:718-23.

[13]. Banan MR, Banan MR, Hjelmstad K. Parameter estimation of structures from static response. I. Computational aspects. Journal of Structural Engineering. 1994;120:3243-58.

[14]. Banan MR, Banan MR, Hjelmstad KD. Parameter Estimation of Structures from Static Response. II: Numerical Simulation Studies. Journal of Structural Engineering. 1994;120:3259-83.

[15]. Viola E, Bocchini P. Non-destructive parametric system identification and damage detection in truss structures by static tests. Structure and Infrastructure Engineering. 2013;9:384-402.

[16]. Ghrib F, Li L, Wilbur P. Damage identification of euler–bernoulli beams using static responses. Journal of Engineering Mechanics. 2011;138:405-15.

[17]. Avril S, Pierron F. General framework for the identification of constitutive parameters from full-field measurements in linear elasticity. International Journal of Solids and Structures. 2007;44:4978-5002.

[18]. Yang Q, Sun B. Structural damage localization and quantification using static test data. Structural Health Monitoring. 2011;10:381-9.

[19]. Rezaiee-Pajand M, Kazemiyan MS, Aftabi. S A. Static damage identification of 3D and 2D frames. Mechanics Based Design of Structures and Machines. 2014;42:70-96.

[20]. Caddemi S, Greco A. The influence of instrumental errors on the static identification of damage parameters for elastic beams. Computers & Structures. 2006;84:1696-708.

[21]. Bakhtiari-Nejad F, Rahai A, Esfandiari A. A structural damage detection method using static noisy data. Engineering Structures. 2005;27:1784-93.

[22]. Ladevèze P, Chouaki A. Application of a posteriori error estimation for structural model updating. Inverse Problems. 1999;15:49.

[23]. Geymonat G, Pagano S. Identification of mechanical properties by displacement field measurement: A variational approach. Meccanica. 2003;38:535-45.

[24]. Florentin E, Lubineau G. Identification of the parameters of an elastic material model using the constitutive equation gap method. Computational Mechanics. 2010;46:521-31.

[25]. Florentin E, Lubineau G. Using constitutive equation gap method for identification of elastic material parameters: technical insights and illustrations. International Journal on Interactive Design and Manufacturing. 2011;5:227-34.

[26]. Lubineau G. A goal-oriented field measurement filtering technique for the identification of material model parameters. Computational Mechanics. 2009;44:591-603.

[27]. Moussawi A, Lubineau G, Florentin E, Blaysat B. The constitutive compatibility method for identification of material parameters based on full-field measurements. Computer Methods in Applied Mechanics and Engineering. 2013;265:1-14.

[28]. Maunder E, De Almeida JM, Ramsay A. A general formulation of equilibrium macro-elements with control of spurious kinematic modes: the exorcism of an old curse. International Journal for Numerical Methods in Engineering. 1996;39:3175-94.

[29]. Wang L, Zhong H. A traction‐based equilibrium finite element free from spurious kinematic modes for linear elasticity problems. International Journal for Numerical Methods in Engineering. 2014;99:763-88.

[30]. Sedaghati R, Suleman A. Force method revisited. AIAA journal. 2003;41:957-66.

[31]. Bonnet M, Constantinescu A. Inverse problems in elasticity. Inverse Problems. 2005;21:R1-R50.

[32]. Celebi M. GPS in dynamic monitoring of long-period structures. Soil Dyn Earthq Eng. 2000;20:477-83.

[33]. Nickitopoulou A, Protopsalti K, Stiros S. Monitoring dynamic and quasi-static deformations of large flexible engineering structures with GPS: Accuracy, limitations and promises. Engineering Structures. 2006;28:1471-82.

[34]. Chen F, Brown GM, Song MM. Overview of three-dimensional shape measurement using optical methods. Opt Eng. 2000;39:10-22.

[35]. Ekstrom MP. Digital image processing techniques: Academic Press; 2012.

[36]. Choi SW, Kim BR, Lee HM, Kim Y, Park HS. A deformed shape monitoring model for building structures based on a 2D laser scanner. Sensors (Basel). 2013;13:6746-58.

[37]. Park HS, Lee HM, Adeli H, Lee I. A new approach for health monitoring of structures: Terrestrial laser scanning. Computer-Aided Civil and Infrastructure Engineering. 2007;22:19-30.

[38]. Nassif HH, Gindy M, Davis J. Comparison of laser Doppler vibrometer with contact sensors for monitoring bridge deflection and vibration. NDT & E International. 2005;38:213-8.

[39]. Hild F, Roux S. Digital image correlation: from displacement measurement to identification of elastic properties - a review. Strain. 2006;42:69-80.

[40]. Jiang R, Jáuregui DV, White KR. Close-range photogrammetry applications in bridge measurement: Literature review. Measurement. 2008;41:823-34.

[41]. Patsias S, Staszewski WJ. Damage Detection Using Optical Measurements and Wavelets. Struct Health Monit. 2002;1:5-22.

[42]. Ji YF, Chang CC. Nontarget image-based technique for small cable vibration measurement. J Bridge Eng. 2008;13:34-42.

[43]. Morlier J, Michon G. Virtual Vibration Measurement Using KLT Motion Tracking Algorithm. Journal of Dynamic Systems, Measurement, and Control. 2010;132:011003.

[44]. Park J-W, Lee J-J, Jung H-J, Myung H. Vision-based displacement measurement method for high-rise building structures using partitioning approach. NDT & E International. 2010;43:642-7.

[45]. Fu G, Moosa AG. An optical approach to structural displacement measurement and its application. Journal of Engineering Mechanics. 2002;128:511-20.

[46]. Choi H-S, Cheung J-H, Kim S-H, Ahn J-H. Structural dynamic displacement vision system using digital image processing. NDT & E International. 2011;44:597-608.

[47]. Jurjo DLBR, Magluta C, Roitman N, Gonçalves PB. Experimental methodology for the dynamic analysis of slender structures based on digital image processing techniques. Mechanical Systems and Signal Processing. 2010;24:1369-82.

[48]. Kim S-W, Kim N-S. Multi-point Displacement Response Measurement of Civil Infrastructures Using Digital Image Processing. Procedia Engineering. 2011;14:195-203.

[49]. Lee JJ, Shinozuka M. A vision-based system for remote sensing of bridge displacement. NDT & E International. 2006;39:425-31.

[50]. Nakamura S. GPS measurement of wind-induced suspension bridge girder displacements. J Struct Eng-Asce. 2000;126:1413-9.

[51]. Park SW, Park HS, Kim JH, Adeli H. 3D displacement measurement model for health monitoring of structures using a motion capture system. Measurement. 2015;59:352-62.

[52]. Wahbeh AM, Caffrey JP, Masri SF. A vision-based approach for the direct measurement of displacements in vibrating systems. Smart Mater Struct. 2003;12:785-94.

[53]. Olaszek P. Investigation of the dynamic characteristic of bridge structures using a computer vision method. Measurement. 1999;25. Epub 236.

[54]. Ladeveze P, Leguillon D. Error estimate procedure in the finite element method and applications. SIAM Journal on Numerical Analysis. 1983;20:485-509.

[55]. Charbonnel P-E, Ladevèze P, Louf F, Le Noac'h C. A robust CRE-based approach for model updating using in situ measurements. Computers & Structures. 2013;129:63-73.

[56]. Widlak T, Scherzer O. Stability in the linearized problem of quantitative elastography. Inverse Problems. 2015;31:035005.

[57]. Lee HM, Park HS. Gage-Free Stress Estimation of a Beam-like Structure Based on Terrestrial Laser Scanning. Computer-Aided Civil and Infrastructure Engineering. 2011;26:647-58.

[58]. Knowles I. Uniqueness for an elliptic inverse problem. SIAM Journal on Applied Mathematics. 1999;59:1356-70.

[59]. Knowles I. Parameter identification for elliptic problems. Journal of Computational and Applied Mathematics. 2001;131:175-94.

[60]. Kohn RV, Lowe BD. A variational method for parameter identification. RAIRO-Modelisation mathématique et analyse numérique. 1988;22:119-58.

[61]. Richter GR. An inverse problem for the steady state diffusion equation. SIAM Journal on Applied Mathematics. 1981;41:210-21.

[62]. Kolda TG, Lewis RM, Torczon V. Optimization by direct search: New perspectives on some classical and modern methods. SIAM review. 2003;45:385-482.

Appendix

This appendix gives detailed proofs of Theorems 1 and 2 and clarifies some important theoretical aspects of the proposed approach.

Proof of Theorem 1.

(a), (b) and (c) are obvious from reference [23].

(d) Denote the minimizer by (M,k), which satisfies the following two conditions,

$$\int_X \frac{M^2}{k^2}\delta\tilde{k}dx = \int_X (w'')^2\delta\tilde{k}dx, \forall \delta\tilde{k} \in \mathrm{C}_0, \tag{25}$$

and

$$\int_X \frac{M}{k}\delta\tilde{M}dx = \int_X w''\delta\tilde{M}dx, \forall \delta\tilde{M} \in \Im_0. \tag{26}$$

Then, contradiction is utilized to verify

$$\mu(x \in X : w''(x) = 0) = 0 \Rightarrow \mu(x \in X : M(x) = 0) = 0. \tag{27}$$

Assume that there exists a subset $X_{pp} \subseteq X$ with $\mu(X_{pp}) > 0$ such that $M(x) = 0$ on X_{pp}. Trivially, substitution of $\delta\tilde{k} = \begin{cases} c, x \in X_{pp} \\ 0, x \in X \setminus X_{pp} \end{cases}, c = \frac{1}{2}(C_0 - c_0) > 0$ into **Eq.** (25) yields

$$\int_{X_{pp}} c(w'')^2 dx = 0 \tag{28}$$

which contradicts with the condition $\mu(w''(x) = 0, x \in X) = 0$.

Next, let $\delta^2_{\tilde{M}}F$ and $\delta^2_{\tilde{k}}F$ denote the second order variations on $F(\cdot,\cdot)$ for $\tilde{M}$ and $\tilde{k}$, respectively. Simple manipulations lead to

$$\begin{aligned} \delta^2_{\tilde{M}}F &= \int_X \frac{(\delta\tilde{M})^2}{\tilde{k}}dx \geq \frac{1}{C_0}\int_X (\delta\tilde{M})^2 dx > 0, \\ \delta^2_{\tilde{k}}F &= \int_X \frac{\tilde{M}^2}{\tilde{k}^3}(\delta\tilde{k})^2 dx \geq \frac{1}{C_0^3}\int_X \tilde{M}^2(\delta\tilde{k})^2 dx > 0 \end{aligned} \tag{29}$$

for $\int_X (\delta\tilde{M})^2 dx > 0$, $\int_X (\delta\tilde{k})^2 dx > 0$ and $\tilde{M} \in \Im^*$, indicating the separately strict convexity on $\Im^* \times \mathrm{C}$.

Remark 1.

From **Eq.** (26), it is found that

$$\int_X \frac{\tilde{M}}{\tilde{k}} \delta\tilde{M} dx = \int_X w'' \delta\tilde{M} dx = \sum\nolimits_p (\theta_p \delta\tilde{M}|_p + w_p (\delta\tilde{M})'|_p) \tag{30}$$

where the subscript *p* indicates the prescribed displacement boundary condition. Obviously, **Eq.** (30) embodies the minimum complementary energy principle

$$M(\tilde{k}) = \arg\min_{\tilde{M}\in\Im} \{\frac{1}{2}\int_X \frac{\tilde{M}^2}{\tilde{k}} dx - \sum\nolimits_p (\theta_p \tilde{M}|_p + w_p (\tilde{M})'|_p)\} \tag{31}$$

and corresponds to a unique mapping $d : \mathrm{C} \to \mathrm{U}$ such that

$$\int_X \tilde{k}\left(d(\tilde{k})\right)'' v'' dx = \int_X q(x) v dx + \sum (F^{ex} v(x^{ex}) + M^{ex} v'(x^{ex})), \forall v \in \mathrm{U}_0 \tag{32}$$

and $M(\tilde{k}) = \tilde{k}\left(d(\tilde{k})\right)''$. With these notations, the minimization problem (7) can become

$$\min_{\tilde{M}\in\Im,\tilde{k}\in\mathrm{C}} F(\tilde{M},\tilde{k}) = \min_{\tilde{k}\in\mathrm{C}} \frac{1}{2}\int_X \frac{(M(\tilde{k}) - \tilde{k}w'')^2}{\tilde{k}} dx = \min_{\tilde{k}\in\mathrm{C}} \frac{1}{2}\int_X \tilde{k}\left|(d(\tilde{k}) - w)''\right|^2 dx, \tag{33}$$

which is a common variational form for inverse identification and its well-posedness has been investigated in a variety of work (see [58-60]for instance). As indicated in the work, problem (33) as well as problem (7) will have a unique minimizer if $\inf_{x\in X} |w''| > 0$ and $\tilde{k}$ is prescribed along the inflow portion of the boundary [61]. It is noted that $\inf_{x\in X} |w''| > 0$ is a stronger version of the *deforming condition* $\mu(x \in X : w''(x) = 0) = 0$.

For proof of Theorem 2, a lemma is introduced first.

Lemma 1

Let $f: H \to \mathbf{R}$ be a continuous and strictly convex function and $u \in H$ be its unique minimizer, where H is a compact Banach space with norm $\|\cdot\|$. Then, for an arbitrary sequence $\{u_n\}_{n=0}^{\infty} \in H$ satisfying $\lim_{n\to\infty} f(u_n) = f(u)$, one has

$$\lim_{n\to\infty} \|u_n - u\| = 0. \tag{34}$$

Proof

This is obvious by contradiction. Assume that $\|u_n - u\|$ does not converge to zero; that is, there exists a positive constant ε such that for an arbitrary positive integer $N > 0$, there is $m \geq N$ with $\|u_m - u\| > \varepsilon$.

Note that $H_\varepsilon = \{v \in H : \|v - u\| \geq \varepsilon\}$ is a compact subspace of H and therefore, f is also continuous and strictly convex on H_ε, implying that there is $u_\varepsilon \in H_\varepsilon$ such that

$$u_\varepsilon = \arg\min_{v \in H_\varepsilon} f(v). \tag{35}$$

By the strict convexity, one has $f(u_\varepsilon) > f(u)$ and hence $f(u_m) \geq f(u_\varepsilon) > f(u)$, contradicting with $\lim_{n\to\infty} f(u_n) = f(u)$.

Proof of Theorem 2.

From the two-step substitution algorithm in **Table 1**, one has for $(M^0, k^0) \in \Im^* \times \mathrm{C}_h$ and the integer $n \geq 0$

$$\begin{aligned} k^{n+1} &= \arg\min_{k \in \mathrm{C}_h} F(M^n, \tilde{k}), \\ M^{n+1} &= \arg\min_{\tilde{M} \in \Im^*} F(\tilde{M}, k^{n+1}). \end{aligned} \tag{36}$$

Then, define a sequence $\{F_n\}_{n=0}^{\infty}$ as

$$F_{2m} = F(M^m, k^m), F_{2m+1} = F(M^m, k^{m+1}), m \in \square \tag{37}$$

and by considering **Eq.** (36), one has

$$F_{2m} \geq F_{2m+1} \geq F_{2m+2}\,. \tag{38}$$

Along with *Theorem 1*(a), it is seen that $F_n \geq 0, n = 0,1,...$ and thus, it is deduced that $\{F_n\}_{n=0}^{\infty}$ is a decreasing and bounded (from below) sequence, meaning that $\{F_n\}_{n=0}^{\infty}$ is a Cauchy sequence. Furthermore, uniqueness of the minimizer must require $(M_h, k_h) \in \mathfrak{I}^* \times \mathrm{C}_h$ and by *Theorem 1*(d), $F(\cdot,\cdot)$ is separately strictly-convex on $\mathfrak{I}^* \times \mathrm{C}_h$. Thus, on considering *Lemma 1*, one has

$$\begin{aligned} &F_{2m+1} - F_{2m} \to 0 \Rightarrow \left\| k^{m+1} - k^m \right\|_{L^2} \to 0, \\ &F_{2m+2} - F_{2m+1} \to 0 \Rightarrow \left\| M^{m+1} - M^m \right\|_{L^2} \to 0. \end{aligned} \tag{39}$$

By further exploiting the information in **Eq.** (36), one has

$$\nabla_{\tilde{k}} F(M^n, k^{n+1}) \cdot \delta\tilde{k} := \int_X [-(\frac{M^n}{k^{n+1}})^2 + (w'')^2]\delta\tilde{k}dx = 0 \tag{40}$$

and

$$\nabla_{\tilde{M}} F(M^{n+1}, k^{n+1}) \cdot \delta\tilde{M} := \int_X (\frac{M^{n+1}}{k^{n+1}} - w'')\delta\tilde{M}dx = 0\,. \tag{41}$$

By continuity, it is inferred from **Eqs.** (40) and (39) that

$$\nabla_{\tilde{k}} F(M^{n+1}, k^{n+1}) \cdot \delta\tilde{k} \to \nabla_{\tilde{k}} F(M^n, k^{n+1}) \cdot \delta\tilde{k} = 0, \text{ as } n \to \infty. \tag{42}$$

Next, it is concluded from **Eqs.** (41) and (42) that

$$\lim_{n\to\infty} \begin{pmatrix} \nabla_{\tilde{M}} F(M^n, k^n) \cdot \delta\tilde{M} \\ \nabla_{\tilde{k}} F(M^n, k^n) \cdot \delta\tilde{k} \end{pmatrix} = \begin{pmatrix} 0 \\ 0 \end{pmatrix} \tag{43}$$

By Taylor expansion [62] at the minimizer (M_h, k_h), one can have

$$\begin{pmatrix} \nabla_{\tilde{M}} F(M^n,k^n)\cdot\delta\tilde{M} \\ \nabla_{\tilde{k}} F(M^n,k^n)\cdot\delta\tilde{k} \end{pmatrix} = \begin{pmatrix} \nabla_{\tilde{M}} F(M_h,k_h)\cdot\delta\tilde{M} \\ \nabla_{\tilde{k}} F(M_h,k_h)\cdot\delta\tilde{k} \end{pmatrix} + \begin{pmatrix} M^n - M_h \\ k^n - k_h \end{pmatrix}^T \cdot J(M_\xi,k_\varsigma)\cdot\begin{pmatrix} \delta\tilde{M} \\ \delta\tilde{k} \end{pmatrix} \quad (44)$$
$$= \begin{pmatrix} M^n - M_h \\ k^n - k_h \end{pmatrix}^T \cdot J(M_\xi,k_\varsigma)\cdot\begin{pmatrix} \delta\tilde{M} \\ \delta\tilde{k} \end{pmatrix}$$

where (M_ξ,k_ς) is the linear interpolation of between (M^n,k^n) and (M_h,k_h), $J(M_\xi,k_\varsigma)$ is the second order Hessian matrix of $F(\cdot,\cdot)$ at (M_ξ,k_ς). Trivially, inserting $\delta\tilde{M} = M^n - M_h$ and $\delta\tilde{k} = k^n - k_h$ into **Eq.** (44) and noticing the fact that $J(M_\xi,k_\varsigma)$ is positive definite due to the strict convexity of $F(\cdot,\cdot)$ in the vicinity of (M_h,k_h), it eventually follows from **Eqs.** (43) and (44) that

$$\lim_{n\to\infty}\left\|M^n - M_h\right\|_{L^2} = 0, \lim_{n\to\infty}\left\|k^n - k_h\right\|_{L^2} = 0. \quad (45)$$

Figure list

Table 1 A two-step substitution algorithm for min-CRE approach under multiple sets of static measurements w

- Given the initial stiffness k^0 and the initial bending moment $M^{(1)0}, M^{(2)0}, \ldots$,

  i.e.

  $M^{(1)0} = Force\_Method(k^0, \Im^{(1)}, \mathrm{U}^{(1)}),$
  $M^{(2)0} = Force\_Method(k^0, \Im^{(2)}, \mathrm{U}^{(2)}),$
  ...

- Successively determine $\left(k^{n+1}, M^{(1)n+1}, M^{(2)n+1}, \ldots\right)$ from $\left(k^n, M^{(1)n}, M^{(2)n}, \ldots\right)$ by

  the following two steps,

  step 1: $k^{n+1} = \{\sqrt{\dfrac{\int_{X_i} \sum_j r_j (M^{(j)n})^2 dx}{\int_{X_i} \sum_j r_j (w^{(j)n})^2 dx}}, x \in X_i, i = 1, 2, \ldots, N\},$

  $M^{(1)n+1} = Force\_Method(k^{n+1}, \Im^1, \mathrm{U}^1),$

  step 2: $M^{(2)n+1} = Force\_Method(k^{n+1}, \Im^2, \mathrm{U}^2),$

  ...

- Test of convergence with given error tolerance TOL,

$$\sqrt{\frac{\int_X (k^{n+1} - k^n)^2 dx}{\int_X (k^0)^2 dx}} + \sqrt{\frac{\int_X (M^{(1)n+1} - M^{(1)n})^2 dx}{\int_X (M^{(1)0})^2 dx}} + \sqrt{\frac{\int_X (M^{(2)n+1} - M^{(2)n})^2 dx}{\int_X (M^{(2)0})^2 dx}} + \ldots \le \mathrm{TOL}$$

Table 2 A two-step substitution algorithm for modified min-CRE approach under multiple sets of static measurements w

- Given the initial stiffness k^0, the initial displacements $w^{(1)0}, w^{(2)0}, \ldots$ and the initial bending moments $M^{(1)0}, M^{(2)0}, \ldots$, i.e.

$$(M^{(1)0}, w^{(1)0}) = recovery(k^0, \Im^{(1)}, \mathrm{U}^{(1)}, \{\hat{w}_i^{(1)}, i \in \wp\}),$$
$$(M^{(2)0}, w^{(2)0}) = recovery(k^0, \Im^{(2)}, \mathrm{U}^{(2)}, \{\hat{w}_i^{(2)}, i \in \wp\}),$$
$$\ldots\ldots$$

- Successively determine $\left(k^{n+1}, M^{(j)n+1}, w^{(j)n+1}\right)$ from $\left(k^n, M^{(j)n}, w^{(j)n}\right)$ by the following two steps,

step 1: $$k^{n+1} = \left\{ \sqrt{\frac{\int_{X_i} \sum_j r_j (M^{(j)n})^2 dx}{\int_{X_i} \sum_j r_j (w^{(j)n''})^2 dx}}, x \in X_i, i = 1, 2, \ldots, N \right\},$$

step 2:
$$(M^{(1)n+1}, w^{(1)n+1}) = recovery(k^{n+1}, \Im^{(1)}, \mathrm{U}^{(1)}, \{\hat{w}_i^{(1)}, i \in \wp\}),$$
$$(M^{(2)n+1}, w^{(2)n+1}) = recovery(k^{n+1}, \Im^{(2)}, \mathrm{U}^{(2)}, \{\hat{w}_i^{(2)}, i \in \wp\}),$$
$$\ldots\ldots$$

- Test of convergence with given error tolerance TOL,

$$\sqrt{\frac{\int_X (k^{n+1} - k^n)^2 dx}{\int_X (k^0)^2 dx}} + \sqrt{\frac{\int_X (M^{(1)n+1} - M^{(1)n})^2 dx}{\int_X (M^{(1)0})^2 dx}} + \sqrt{\frac{\int_X (M^{(2)n+1} - M^{(2)n})^2 dx}{\int_X (M^{(2)0})^2 dx}} + \ldots$$
$$+ \sqrt{\frac{\int_X (w^{(1)n+1} - w^{(1)n})^2 dx}{\int_X (w^{(1)0})^2 dx}} + \sqrt{\frac{\int_X (w^{(2)n+1} - w^{(2)n})^2 dx}{\int_X (w^{(2)0})^2 dx}} + \ldots \le \mathrm{TOL}$$

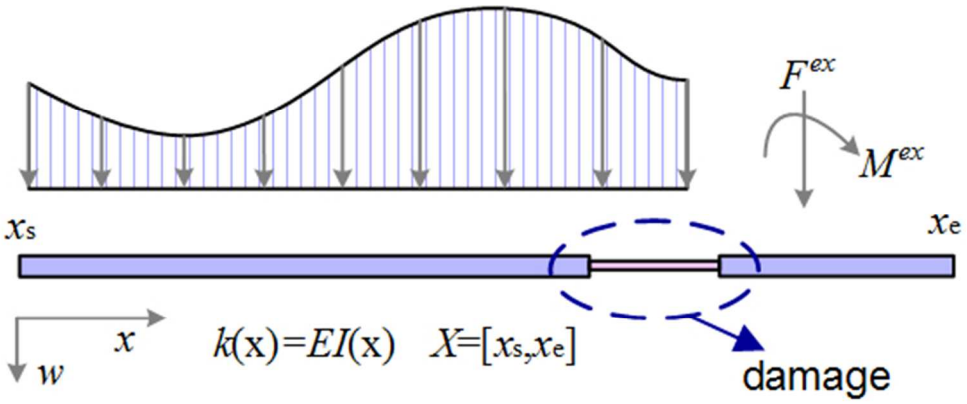

Fig. 1 A Bernoulli-Euler beam with damage

76x31mm (192 x 192 DPI)

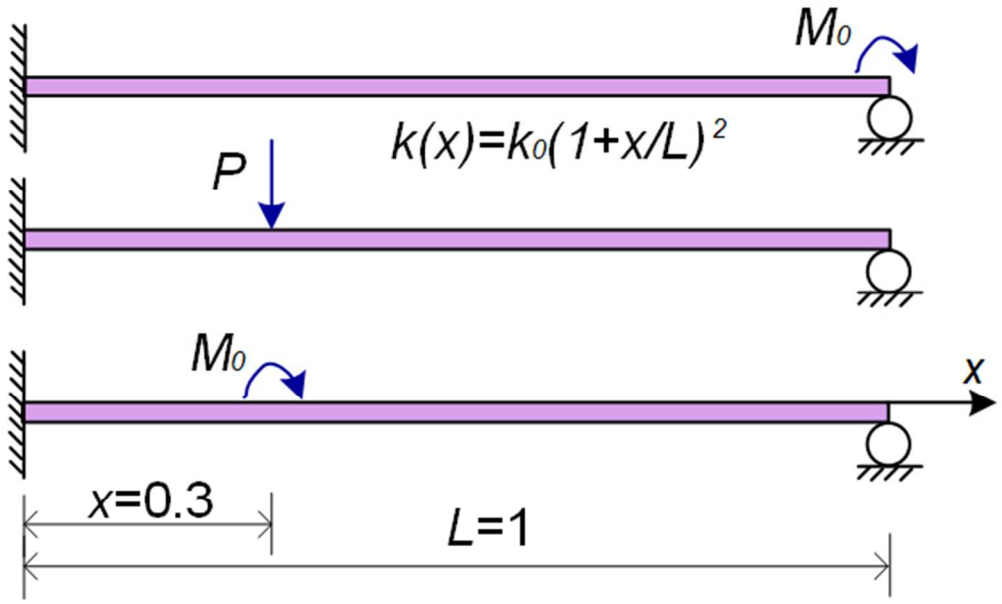

Fig. 2 Geometry and loads for a propped cantilever beam

82x50mm (192 x 192 DPI)

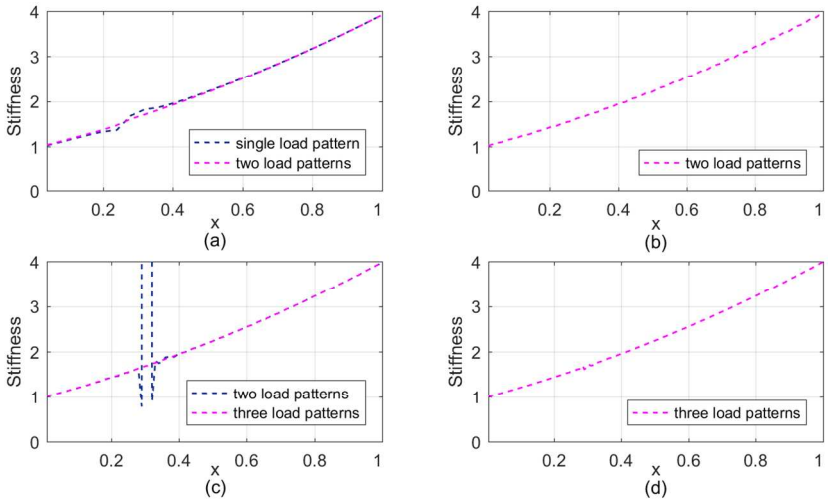

Fig. 3 Damage identifications in propped cantilever beam: (a) 25 elements under single load pattern and two load patterns, (b) 50 elements under two load patterns, (c) 100 elements under two loads pattern and three load patterns and (d) 200 elements under three load patterns

419x221mm (96 x 96 DPI)

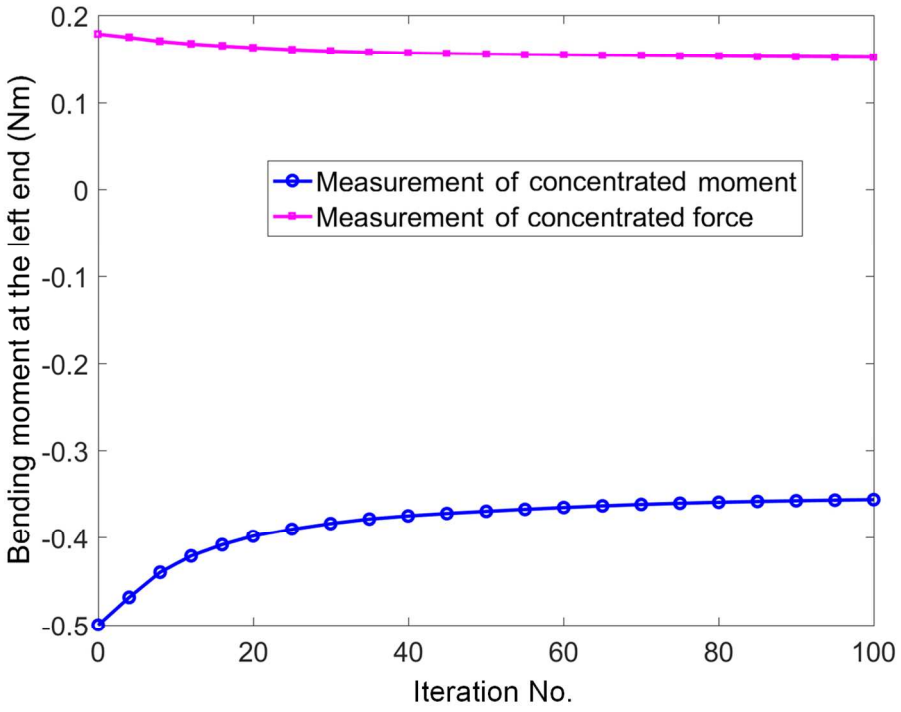

Fig. 4 Convergence of bending moment at left end of propped cantilever beam

203x155mm (192 x 192 DPI)

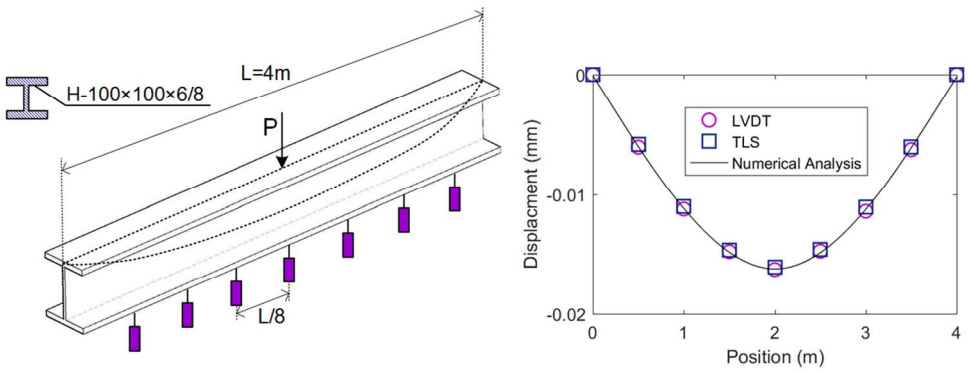

Fig. 5 Geometry and experimental displacements of simply supported beam

177x64mm (192 x 192 DPI)

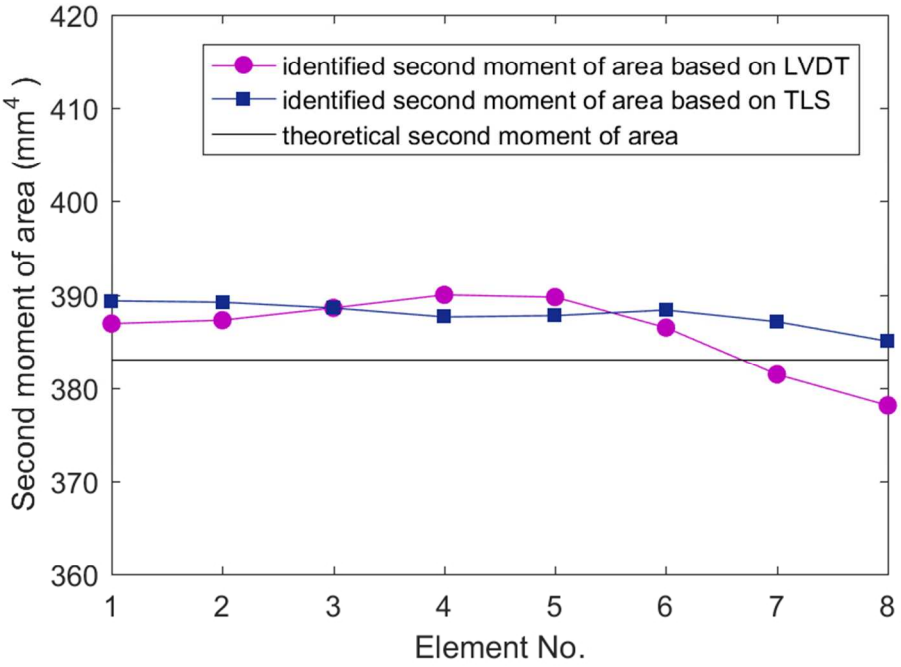

Fig. 6 Second moment of area identified by modified min-CRE approach comparing to the theoretical second moment of area of simply supported beam

246x173mm (96 x 96 DPI)

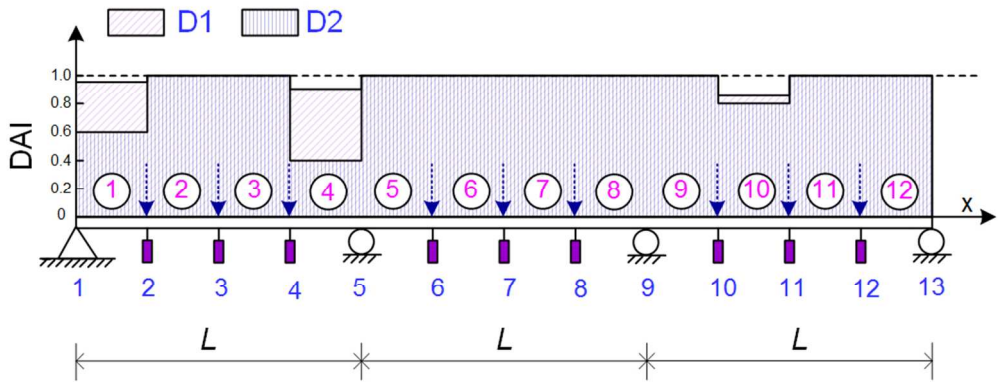

Fig. 7 Geometry, damage location and load cases of three-span continuous beam (D1-damage case 1, D2-damage case 2)

140x53mm (192 x 192 DPI)

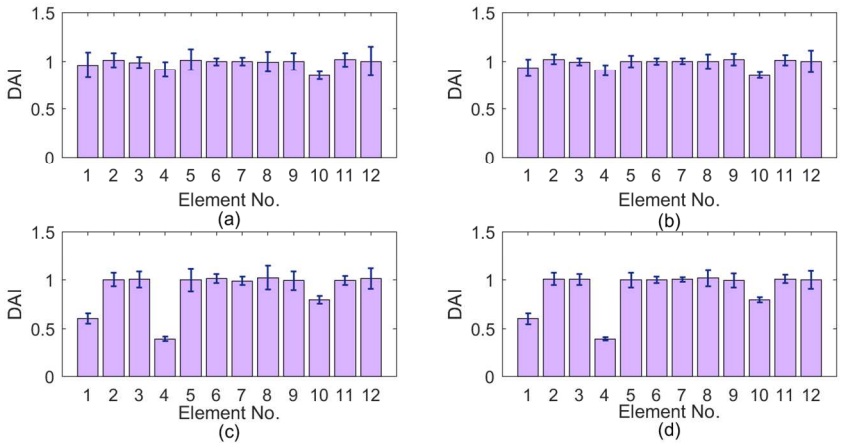

Fig. 8 Mean values and standard deviations of DAI with 0.1mm noise for: (a) small damage case D1 by min-CRE approach, (b) small damage case D1 by modified min-CRE approach, (c) large damage case D2 by min-CRE approach, (d) large damage case D2 by modified min-CRE approach.

414x192mm (96 x 96 DPI)

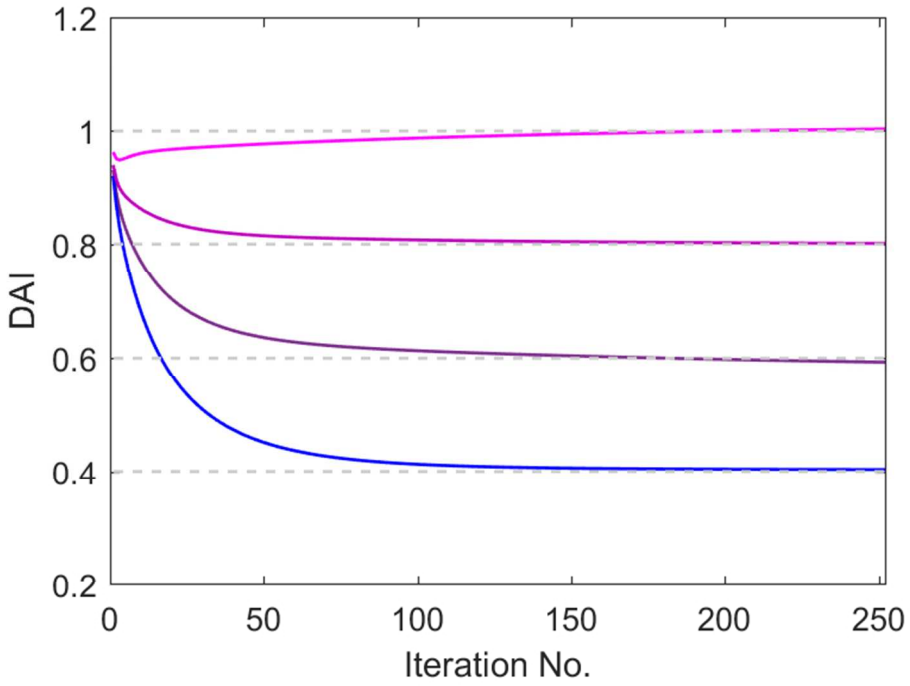

Fig. 9 Convergence of the damage indices of three-span continuous beam under D1

222x160mm (96 x 96 DPI)

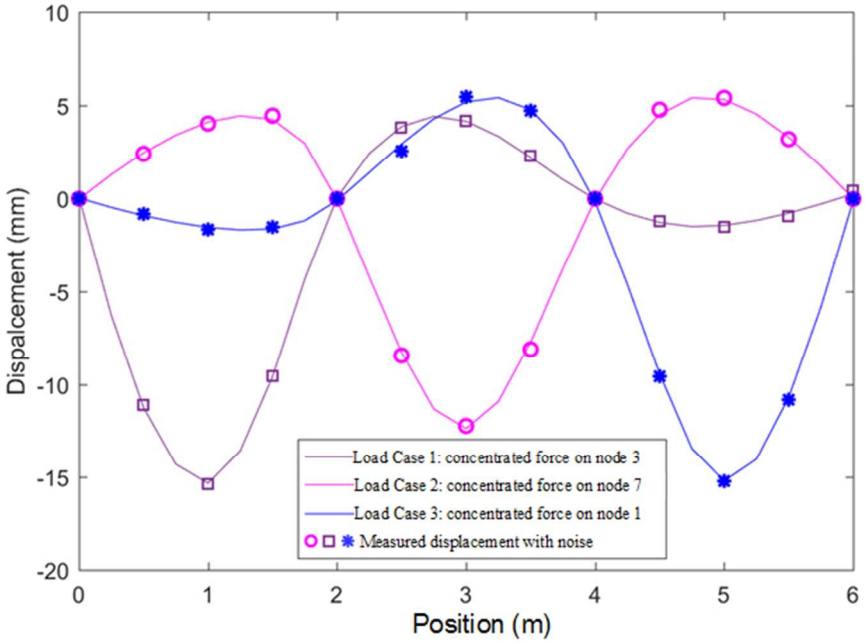

Fig. 10 Displacement fields rebuilt by modified min-CRE approach comparing to the displacement boundary.

94x65mm (192 x 192 DPI)